03

Visualization of Thermal Fields Evolution During Shock Wave Reflection From a Shock Channel End

© I.A. Znamenskaya, M.I. Muratov

Moscow State University, Moscow, Russia
E-mail: muratov583@gmail.com

Received May 29, 2023
Revised June 14, 2023
Accepted June 14, 2023

Panoramic thermographic visualization of a non-stationary thermal fields on the rectangular shock tube end wall was carried out. Thermal fields evolution of outer (end wall) surface during shock wave reflection is studied. Heat fluxes distribution data were obtained at various times within 4 seconds after reflection. The influence of the boundary layer on heat transfer behind the reflected shock wave is analyzed

Keywords: Reflected shock wave, Shock tube, Non-stationary heat flux, Infrared thermography.

DOI: 10.61011/TPL.2023.08.56695.19643

In a one-dimensional model, the state of gas behind a plane shock wave reflected off a rigid wall is characterized by constant thermodynamic parameters derived from conservation laws. In the real world, the reflected from a wall shock wave propagates in a channel through a nonuniform flow consisting of a core flow and a boundary layer formed behind the incident shock wave. Perturbations in a nonuniform flow field in front of the reflected shock induce the formation of a time-varying nonuniform field of gas-dynamic parameters behind the reflected shock wave [1]. Boundary-layer effects trigger a spatial redistribution of the velocity, temperature, and density behind the reflected wave. Notably, this needs to be taken into account in chemical kinetics experiments [2]. The formation of a viscous dynamic boundary layer [3] has an impact on fast growth of the boundary thermal layer [4]. For sufficiently thin walls of experimental shock tubes, it requires to consider the nonadiabaticity of processes involving heat exchange at the interface between gas and the external (relative to a text stand) environment.

Complex problems of this kind are normally solved in experiments through the use of various types of heat flux probes (specifically, those relying on the Seebeck effect [5–7]). However, while these methods have a considerably good temporal resolution, they do not provide an exhaustive evolution coverage of heat flux fields. In the three-dimensional case, the correlation between the considered phenomena in a channel with a reflected shock wave and the corresponding local measurements is rather complex.

In the present study, the dynamics of thermal fields of an outer end surface of a channel is visualized using high-speed infrared thermography. This visualization provides an opportunity to examine non-stationary heat fluxes with strong spatial gradients of measured quantities [8]. Although the absolute measurement error is fairly large, obtained data on the continuous distribution of thermal radiation intensity provide new information regarding the flow field that cannot be retrieved by simple interpolation of a finite amount of data of point measurements [9].

The aim of the study is to perform a panoramic investigation of heat fluxes at the end face of a gas-dynamic test stand and analyze the influence of the boundary layer on heat exchange behind a reflected shock wave via high-speed infrared thermography. Experiments were carried out at an UTRO-3 shock test stand (single-diaphragm shock tube). The high-pressure chamber was separated from the low-pressure one with a rectangular cross section (24×48 mm) by a thin polymer diaphragm (Fig. 1). The length of high- and low-pressure chambers was 52 and 211 cm, and the thickness of copper walls was 2 mm. Air and helium were driven and driver gases, respectively. Piezoelectric pressure sensors, which were used to measure the shock wave velocity (element A in Fig. 1), were mounted along the low-pressure chamber. An insert (stainless-steel plate 0.25 mm in thickness; element C in Fig. 1) was mounted at the end of the low-pressure chamber.

A high-speed cooled high-resolution infrared receiver (FLIR SC 7700 with an operating range of $3.7-4.8\,\mu$m) was used as a thermal radiation detector. Varying the spatial resolution of the camera (up to 160×128 px), it was possible to alter the time resolution and measure heat fluxes at a frame rate up to 925 fps; the integration time was set to 1 ms. Heat fluxes were measured at the outer surface of the insert (Fig. 1). The thermal imager (element E in Fig. 1) was mounted horizontally at a distance of 20–30 cm from the tube end and at angle $\alpha \approx 13^\circ$ to the major axis of the shock tube (to avoid potential damage to the detector. In order to raise signal-to-noise ratio and suppress the influence of background radiation, the emissivity of the detection region was enhanced as much as possible by coating the outer surface of the insert with a thin layer of black acrylic paint. In the thermal imager settings, the emissivity was set to $\varepsilon = 0.95$.

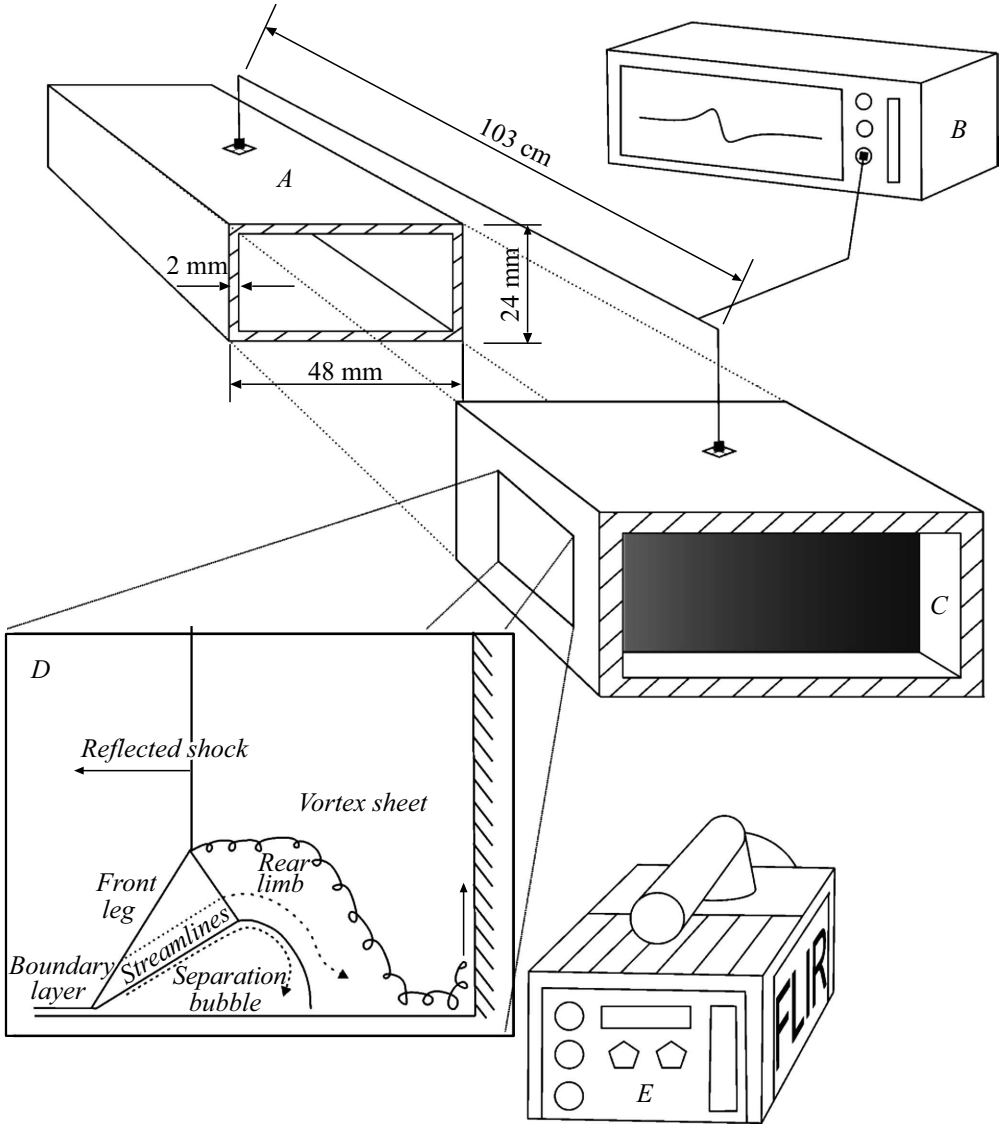

Figure 1. Schematic diagram of the experimental setup. *A* — Piezoelectric pressure sensors, *B* — oscilloscope receiving the signal from pressure sensors, *C* — insert at the end of the low-pressure chamber (211 cm away from the diaphragm), *D* — flow diagram for a reflected shock wave, and *E* — FLIR SC 7700 thermal imaging camera.

A boundary gas layer forms and grows behind the front of an incident shock wave. This process is caused by the interaction of a flow and wall by means of viscosity and thermal conductivity, which leads to a gas parameters nonuniformity over the cross section of the tube channel. Under normal reflection of a shock wave off a plane end wall, the motion of a reflected shock wave has distinctive features related to the presence of a boundary layer behind the incident shock wave. Regimes emerging in this case may be such that the propagation of a reflected shock over the flux core and the boundary layer (the perimeter) will result in splitting of the reflected wave with the formation of λ-configurations near the walls (diagram *D* in Fig. 1). It should be noted that the characteristic sizes of the formed bifurcation configuration might be significantly larger than the thickness of the boundary layer [10]. The formation of such bifurcation structures is related to the inflow of a part of the boundary layer into the stagnant zone due to a pressure difference between the reflected wave and the deceleration zone in the boundary layer. As the stagnant zone increases in volume, the height of the triple point of the bifurcation configuration also increases.

Moving away from the reflection surface, a structured shock leaves behind a near-wall layer of rapidly turbulizing gas with an unsteady vortex sheet, which forms a non-stationary heat flux on the end wall (diagram *D* in Fig. 1) [11]. Thus, temperature fields along the perimeter of the end face after reflection are formed by a well-developed turbulent boundary layer.

A varying heat flux field aligned with the time of motion of the reflected shock wave away from the end face is produced at the outer side of the reflection surface. Owing

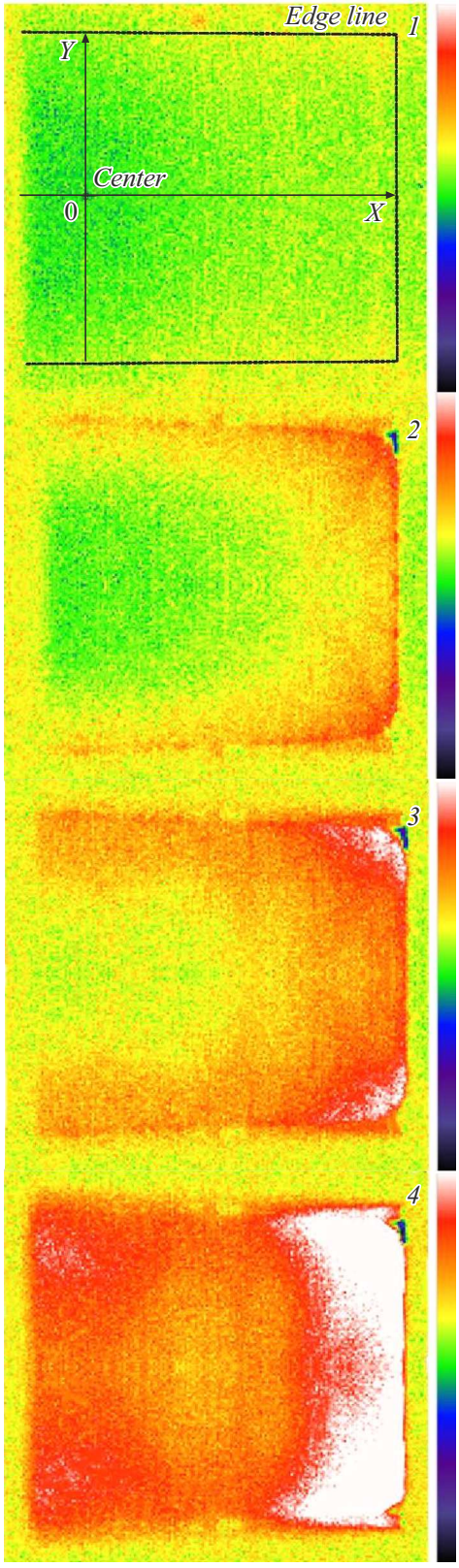

Figure 2. Two-dimensional thermal fields representing the reflection of a shock wave off the end of the shock tube channel within a region 24×24 mm in size at the following time points: 0 (*1*), 0.02 (*2*), 0.04 (*3*), and 0.1 s (*4*). Images are flipped horizontally along section $(X, 0)$.

to the growth of the boundary layer near the side walls, the heat flux at the channel boundaries is more intense than the one in regions corresponding to heat exchange between the center of the channel end wall and the flux core. The direct heat exchange between the gas medium behind the reflected wave and the outer surface of the end wall is effected primarily via thermal conductivity [9]. Figure 2 presents the result of thermal-imaging visualization of the thermal field of the outer side of the channel end wall at various time points after reflection of a shock wave with Mach number $M = 1.5$ of the incident wave. Prior to wave reflection, the surface of the end wall is characterized (with a correction for the camera angle) by a fairly uniform thermal field (fragment *1* in Fig. 2). The reflection of a shock wave produces a thermal pulse that is carried via thermal conductivity to the outer surface of the end wall. The temperature behind the reflected wave inside the channel was estimated at $T \approx 500$ K. The corresponding change in the measured surface thermal fields is illustrated by Fig. 2 (fragment *2*). The field in different flow regions (flux core and boundary zones near the channel walls) is seen to be nonuniform; the heat-exchange intensity at the boundaries of the insert is higher than the one in central regions. Specifically, the temperature field of the central region remains almost unchanged within the first millisecond after shock-wave reflection, while local heat fluxes in the boundary regions get enhanced due to the intensification of heat exchange by the expanding turbulent wall flux. The central part of the end wall is heated in $t = 0.04$ s from the onset of evolution of heat fluxes of the outer surface of the insert (fragment *3* in Fig. 2). The time-varying transition boundary between regions is visualized. The horizontal transition boundary is more pronounced due to the overlap and merging of boundary layers in the channel (at the vertical wall with its height less than its width). Owing to the fusion of vertical and horizontal turbulent boundary layers throughout the entire near-wall flow in the channel at $t = 0.1$ s (fragment *4* in Fig. 2), the entire examined region undergoes inhomogeneous heating of several degrees, the greater the distance from the channel center.

The quantitative evolution of the temperature field distribution relative to the initial unperturbed surface state (fragment *1* in Fig. 2) along axis $(X, 0)$ is presented in Fig. 3, *a*. The maximum measured temperature difference between the edge and the center of the surface is $\Delta T = 1.5 \pm 0.1$ K, and the maximum difference for the measured temperature at the edge of the end wall is $\Delta T = 3.5 \pm 0.3$ K. The heat flux to the end wall stabilizes within $t \approx 1$ s (with subsequent weakening throughout the entire imaged area). A well-pronounced temperature peak in the region of the vertical edge of the end wall is smoothed out within $t \approx 3-4$ s (Fig. 3, *b*) and becomes level with the flux core values. A dip of the curve at the channel edge (*Leakage* in Fig. 3, *b*) at late times is attributable to the emerging end-type leakage at the joint of planes and local cooling (Van der Waals expansion).

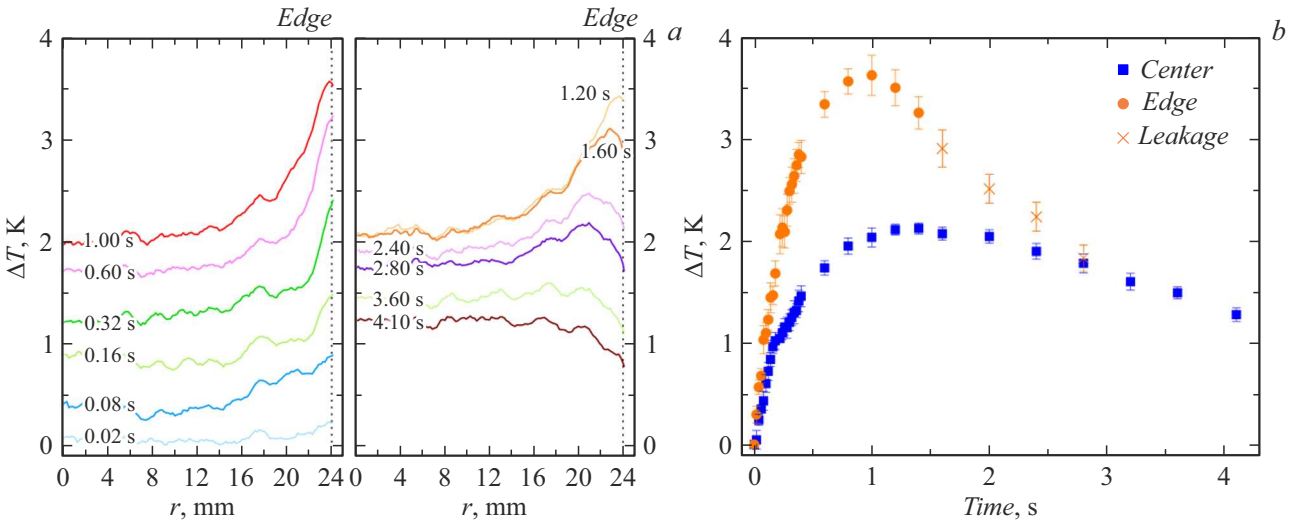

Figure 3. *a* — Variation of temperature from the center (0, 0) to the wall in the channel symmetry plane on the insert, section (X, 0) for different time points; *b* — time dependence of the temperature variation at the center and on the edge of section (X, 0) of the insert.

Non-stationary heat transfer through channel walls is one of the major causes of attenuation of both incident and reflected shock waves, inducing a divergence of theoretical estimates of attenuation obtained without regard to the heat transfer effects for the „viscous“ solution of problems on flow in shock tubes. The issue of heat transfer from hot gas behind a shock wave to channel walls is rather important, but has not been solved completely for relevant Mach numbers of a shock wave. The possibility of verification of the results of numerical calculations against thermographic temperature fields of surfaces of gas-dynamic test stands appears to be crucial for the examination of processes in gas-dynamic channels and in the boundary layers of near-wall regions.

Funding

This study was supported financially by the Russian Science Foundation (grant No. 22-29-00652).

Conflict of interest

The authors declare that they have no conflict of interest.

References

[1] G. Ben-Dor, *Shock wave reflection phenomena* (Springer, Berlin–Heidelberg, 2007), p. 49.
[2] E.L. Petersen, R.K. Hanson, Shock Waves, **10** (6), 407 (2001). DOI: 10.1007/PL00004051
[3] R.A. Hartunian, A.L. Russo, P.V. Marrone, J. Aerosp. Sci., **27** (8), 587 (1960). DOI: 10.2514/8.8656
[4] C. Frazier, M. Lamnaouer, E. Divo, A. Kassab, E. Petersen, Shock Waves, **21** (1), 11 (2011). DOI: 10.1007/s00193-010-0282-y
[5] H. Knauss, T. Roediger, D.A. Bountin, B.V. Smorodsky, A.A. Maslov, J. Srulijes, J. Spacecr. Rockets, **46** (2), 255 (2009). DOI: 10.2514/1.32011
[6] Yu.V. Dobrov, V.A. Lashkov, Tech. Phys., **67** (9), 1137 (2022). DOI: 10.21883/TP.2022.09.54676.39-22.
[7] P.A. Popov, N.A. Monakhov, T.A. Lapushkina, S.A. Poniaev, Tech. Phys., **67** (9), 1144 (2022). DOI: 10.21883/TP.2022.09.54677.54-22.
[8] G.M. Carlomagno, G. Cardone, Exp. Fluids, **49** (6), 1187 (2010). DOI: 10.1007/s00348-010-0912-2
[9] I.A. Znamenskaya, E.Yu. Koroteeva, M.I. Muratov, L.S. Shtemenko, O.I. Dokunina, N.N. Sysoev, Moscow Univ. Phys. Bull., **77**, 914 (2022). DOI: 10.3103/S0027134922060145.
[10] T.V. Bazhenova, L.G. Gvozdeva, Yu.P. Lagutov, V.N. Lyakhov, Yu.M. Faresov, V.P. Fokeev, *Nestatsionarnye vzaimodeistviya udarnykh i detonatsionnykh voln v gazakh* (Nauka, M., 1986), p. 119 (in Russian).
[11] H. Kleine, V.N. Lyakhov, L.G. Gvozdeva, H. Grönig, in *Shock waves*, ed. by K. Takayama (Springer, Berlin–Heidelberg, 1992), p. 261. DOI: 10.1007/978-3-642-77648-9_36

Translated by D.Safin